The Astrophysical Journal Letters, 901:L30 (5pp), 2020 October 1 https://doi.org/10.3847/2041-8213/abb886

The Archetypal Ultra-diffuse Galaxy, Dragonfly 44, Is not a Dark Milky Way

Ákos Bogdán
Harvard-Smithsonian Center for Astrophysics, 60 Garden Street, Cambridge, MA 02138, USA; abogdan@cfa.harvard.edu
Received 2020 September 7; revised 2020 September 13; accepted 2020 September 14; published 2020 September 28

Abstract

Due to the peculiar properties of ultra-diffuse galaxies (UDGs), understanding their origin presents a major challenge. Previous X-ray studies demonstrated that the bulk of UDGs lack substantial X-ray emission, implying that they reside in low-mass dark matter halos. This result, in concert with other observational and theoretical studies, pointed out that most UDGs belong to the class of dwarf galaxies. However, a subset of UDGs is believed to host a large population of globular clusters (GCs), which is indicative of massive dark matter halos. This, in turn, hints that some UDGs may be failed $L_\star$ galaxies. In this work, I present Chandra and XMM-Newton observations of two archetypal UDGs, Dragonfly 44 and DF X1, and I constrain their dark matter halo mass based on the X-ray emission originating from hot gaseous emission and from the population of low-mass X-ray binaries residing in GCs. Both Dragonfly 44 and DF X1 remain undetected in X-rays. The upper limits on the X-ray emission exclude the possibility that these galaxies reside in massive ($M_{\rm vir} \gtrsim 5 \times 10^{11}\,M_\odot$) dark matter halos, suggesting that they are not failed $L_\star$ galaxies. These results demonstrate that even these iconic UDGs resemble to dwarf galaxies with $M_{\rm vir} \lesssim 10^{11}\,M_\odot$, implying that UDGs represent a single galaxy population.

Unified Astronomy Thesaurus concepts: Active galactic nuclei (16); X-ray astronomy (1810); X-ray sources (1822); Dwarf galaxies (416); Galaxies (573); Galaxy dark matter halos (1880); Galaxy formation (595); Supermassive black holes (1663)

1. Introduction

The physical characteristics of ultra-diffuse galaxies (UDGs) signify that they may represent a new class of galaxies: their surface brightness is extremely low ($\mu_0(g) \gtrsim 24$ mag arcsec^{-2}) and is similar or lower than that of dwarf galaxies, but their effective radius ($r_{\rm eff} \gtrsim 1.5$ kpc) is comparable to more massive galaxies, such as the Milky Way (e.g., Sandage & Binggeli 1984; Schombert et al. 1992; van Dokkum et al. 2015). In addition, stellar kinematics measurements and the discovery of an abundant population of globular clusters (GCs) around some UDGs hinted that UDGs may be the relics of massive galaxies, so-called failed $L_\star$ galaxies (van Dokkum et al. 2016, 2017). However, owing to the demanding nature of deep optical follow-up measurements, only a handful of UDGs were studied in detail, which would support this exotic formation scenario. The alternative formation scenario, favored by several theoretical studies, suggested that UDGs belong to the class of dwarf galaxies, and their large spatial extent is due to energetic stellar feedback (e.g., Amorisco & Loeb 2016; Di Cintio et al. 2017).

The crucial observational difference between these formation scenarios is the dark matter halo mass of UDGs. If UDGs are failed $L_\star$ galaxies, they will reside is massive dark matter halos ($M_{\rm vir} \gtrsim 5 \times 10^{11}\,M_\odot$). If, however, they are genuine dwarf galaxies, they will live in a dwarf-size dark matter halos ($M_{\rm vir} \lesssim 10^{11}\,M_\odot$). Recently, we explored a statistically significant sample of UDGs in isolated and in galaxy cluster environments and constrained their dark matter halo mass using X-ray observations (Kovács et al. 2019, 2020). These studies demonstrate that the bulk of UDGs do not reside in massive dark matter halos, and strengthen the picture, in which UDGs are puffed-up dwarf galaxies. However, due to the statistical nature of these studies, it could not be excluded that a small subset of UDGs resides in massive dark matter halos, implying that UDGs could form via multiple channels.

The most likely candidate UDGs with massive dark matter halos are Dragonfly 44 (hereafter DF 44) and DF X1, which were studied in extensive follow-up campaigns. Deep optical observations suggest the existence of a substantial GC population around these galaxies, which is indicative of massive dark matter halos (van Dokkum et al. 2016, 2017, 2019). In this picture, it is expected that UDGs will exhibit X-ray emission originating from the population of low-mass X-ray binaries (LMXBs) residing in GCs and from diffuse gaseous emission. This X-ray emission should be observable by present-day X-ray telescopes, such as Chandra or XMM-Newton. Both of these galaxies were subject to deep X-ray observations, which allow the detailed investigations of their X-ray emitting properties.

Recently, Lee et al. (2020) studied the ultraviolet and X-ray properties of a sample of UDGs in the Coma cluster that were discovered by the Dragonfly Telephoto Array (Abraham & van Dokkum 2014). They concluded, in agreement with Kovács et al. (2020), that the bulk of UDGs do not exhibit statistically significant X-ray emission. In addition, they analyzed the XMM-Newton data of DF 44 and did not detect statistically significant unresolved emission. In this work, I present deep, high-angular resolution Chandra observations of DF 44, the data of which can resolve LMXBs associated with GCs or a nuclear X-ray source. Based on the Chandra data, I also constrain the X-ray luminosity originating from diffuse gaseous emission and from the population of unresolved X-ray binaries. In addition, I present the XMM-Newton data available for DF X1, and constrain the X-ray luminosity associated with this UDG. Overall, this study aims to fill the missing gap in our understanding about the formation scenarios of UDGs, to directly address whether the most well-studied UDGs could be failed $L_\star$ galaxies, and to probe whether UDGs may have multiple formation channels.

For the distance of DF 44 and DF X1 I assumed $D = 103$ Mpc, at which distance $1''$ corresponds to

Table 1
The List of Analyzed Chandra Observations

Obs ID	$T_{\rm obs}$ (ks)	$T_{\rm filt}$ (ks)	Instrument	Date
20612	29.7	22.8	ACIS-I	2018 Apr 5
21068	33.1	29.5	ACIS-I	2018 Apr 6
21069	32.6	23.7	ACIS-I	2018 Apr 8

0.476 kpc. The Galactic absorption toward Coma cluster is $9.3 \times 10^{19}\,{\rm cm}^{-2}$ (HI4PI Collaboration et al. 2016). Throughout this Letter I used standard Λ-CDM cosmology with $H_0 = 71\,{\rm km\,s^{-1}\,Mpc^{-1}}$, $\Omega_M = 0.3$, and $\Omega_\Lambda = 0.7$.

This Letter is structured as follows. In Section 2 I describe the analysis of Chandra and XMM-Newton data. I present the results in Section 3 and place these results in context in Section 4.

2. Data Analysis

2.1. Chandra

Chandra observed DF 44 in three ACIS-I pointings for a total exposure time of 95.4 ks. The data were analyzed using standard CIAO (version 4.12) tools with CALDB 4.9.1.

The main steps of the analysis are similar to those outlined in Kovács et al. (2020). First, I reprocessed the individual observations with the `chandra_repro` task. To filter high background time periods, I binned the light curves into 200 s bins and excluded those bins that were 2σ above the mean count rates. The original and filtered exposure times are listed in Table 1. The total clean exposure time is 76.0 ks.

In this work, I study the combined emission originating from hot gas and the population of LMXBs. Therefore, I carry out the analysis in the 0.5–8 keV band (see Section 2.3 for details). To this end, I created exposure maps that reflect the spectrum of both of these components by utilizing the combination of an APEC model with $kT = 0.2$ keV temperature and metallicity of $Z = 0.2 Z_\odot$ (Bogdán & Gilfanov 2011; Goulding et al. 2016) and a power-law model with a slope of $\Gamma = 1.56$ (Irwin et al. 2003). Finally, I identified point sources following the procedure of Kovács et al. (2020). For the study of the diffuse emission, these point sources were excluded.

To account for the background emission, I utilized a local background region around DF 44. This approach assures that not only are the instrumental and sky background components accounted for, but the large-scale emission from the Coma cluster is as well. However, this latter component does not play a major role as the emission from the intracluster emission is relatively low at a projected distance of $\sim 1^\circ$ (or 1.7 Mpc) from the core of the Coma cluster.

2.2. XMM-Newton

DF 44 was targeted by two XMM-Newton observations for a total of 164.5 ks. Due to the large field of view of XMM-Newton, one of the observations (ObsID: 0800580201) also includes DF X1. However, I note that DF X1 is at the edge of the detector, implying that the effective exposure time is significantly decreased due to vignetting effects. I combined data from the EPIC-PN and the two EPIC-MOS cameras to maximize the signal-to-noise ratios. The data analysis was carried out following Kovács et al. (2019) using the Science Analysis System software package.

Table 2
The List of Analyzed XMM-Newton Observations

Obs ID	$T_{\rm obs}$[a] (ks)	$T_{\rm filt}$[a] (ks)	Date
0800580101	78.9/78.8/77.3	59.1/61.7/53.4	2017 Dec 23
0800580201	85.6/85.6/84.0	50.8/54.6/29.2	2018 Jan 4

Note.
[a] The exposure times are given for EPIC MOS1, MOS2, and PN.

The first step of the analysis was to exclude high background periods using a two step approach. First, I excluded flares using the 12–14 keV band, which was then followed with filtering any residual flares in the 0.3–10 keV band. To this end, a 2σ filtering was applied for both energy ranges. The effective exposure times are listed in Table 2. In addition, I excluded the out-of-time events, and those events that are at the border of the charge-coupled devices. Throughout the analysis, only pattern zero events were utilized for all three cameras. I identified luminous point sources and excluded them from the analysis of the UDGs. The exposure maps were created in the 0.5–8 keV band.

2.3. Predicted X-Ray Emission from DF 44 and DF X1

The overall X-ray emission observed from galaxies originates from a multitude of sources. The most notable contributions arise from X-ray binaries and truly diffuse gaseous emission, while other X-ray emitting components (such as accreting white dwarves or coronally active binaries) play a lesser role (Gilfanov 2004; Revnivtsev et al. 2007; Bogdán & Gilfanov 2008, 2011; Zhang et al. 2011).

Due to their low star formation rates, DF 44 and DF X1 are not expected to host a substantial population of high-mass X-ray binaries (Lee et al. 2020). Given the low stellar mass ($M_\star \sim 3 \times 10^8\,M_\odot$) of DF 44 and DF X1 (van Dokkum et al. 2019), these galaxies are also not expected to host a large number of LMXBs that were formed through the primordial channel. According to the LMXB luminosity function of Gilfanov (2004), the total expected X-ray luminosity from these LMXBs is $\sim 2.4 \times 10^{37}\,{\rm erg\,s^{-1}}$. However, the population of LMXBs in GCs formed through dynamical interaction is expected to provide a substantial contribution given the large GC population of UDGs. Based on the luminosity function of GC-LMXBs (Zhang et al. 2011) and the number of GCs in DF 44 and DF X1, a luminosity of $4.3 \times 10^{39}\,{\rm erg\,s^{-1}}$ and $3.5 \times 10^{39}\,{\rm erg\,s^{-1}}$ is expected, respectively.

Emission from the hot gas is also expected to be significant for galaxies with massive dark matter halos. Because DF 44 and DF X1 are believed to reside in $M_{\rm vir} \sim 5 \times 10^{11}\,M_\odot$ dark matter halos, based on the $L_{\rm X}$–$M_{\rm tot}$ relation (Kim & Fabbiano 2013; Babyk et al. 2018), we expect the gaseous component to have an X-ray luminosity of $1.8 \times 10^{39}\,{\rm erg\,s^{-1}}$.

Thus, the total expected X-ray emission from DF 44 and DF X1 is $6.1 \times 10^{39}\,{\rm erg\,s^{-1}}$ and $5.3 \times 10^{39}\,{\rm erg\,s^{-1}}$, respectively.

3. Results

3.1. Images

In Figure 1, the 0.5–8 keV band Chandra and XMM-Newton X-ray images of DF 44 are presented. These images do not show a luminous X-ray glow, originating from the population

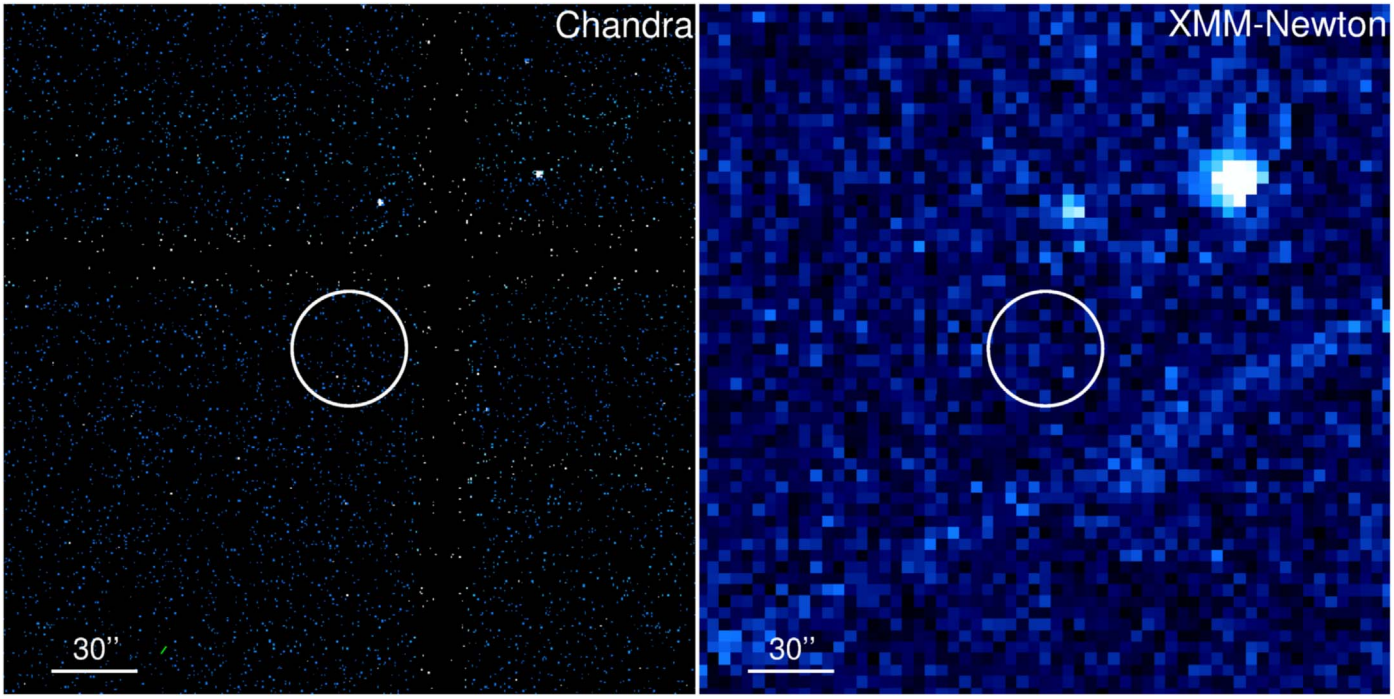

Figure 1. 0.5–8 keV band exposure corrected Chandra (left panel) and XMM-Newton (right panel) images of a $4' \times 4'$ region around DF 44. No diffuse X-ray emission, originating from hot gaseous emission and/or the population of unresolved X-ray binaries, is detected. In addition, no resolved X-ray sources are detected either from GC-LMXBs or from a nuclear source. The lack of statistically significant X-ray emission implies that the dark matter halo of DF 44 is not comparable with $L_\star$ galaxies.

of unresolved LMXBs and from truly diffuse gaseous emission, associated with the UDG. In addition, no bright point sources are associated with the galaxy.

The non-detection of luminous X-ray emission suggests that the luminosity of the X-ray emission associated with the UDGs remains below the detection threshold.

3.2. X-Ray Point Sources

Thanks to the sensitive Chandra and XMM-Newton observations, luminous X-ray point sources, such as an active galactic nucleus (AGN) or LMXBs, can be resolved in and around DF 44. To estimate the source detection sensitivity, I assume five and 20 net counts as the detection threshold for Chandra and XMM-Newton, respectively. Using a typical power-law spectrum with a slope of $\Gamma = 1.56$, the source detection sensitivities are $L_{0.5\text{–}8\,\mathrm{keV}} = 8 \times 10^{38}\,\mathrm{erg\,s^{-1}}$ and $L_{0.5\text{–}8\,\mathrm{keV}} = 4 \times 10^{38}\,\mathrm{erg\,s^{-1}}$, for Chandra and XMM-Newton, respectively. Given the luminosity function of LMXBs, this allows the detection of low-luminosity AGN and bright LMXBs.

The X-ray images of DF 44 do not reveal any luminous X-ray sources in the vicinity of the UDG (Figure 1). The search detection tools also did not detect a luminous X-ray source either in the center or in the halo of DF 44. Based on the X-ray luminosity function of GC-LMXBs, it is expected that the brightest LMXBs could be individually resolved. Given the Chandra and XMM-Newton source detection thresholds and the LMXB luminosity function established in Zhang et al. (2011), it is expected that ∼0.001 and ∼0.005 GC-LMXBs will be detected per GC, respectively. Since DF 44 hosts about 74 GCs, the detection of 0.074 and 0.37 GC-LMXBs is detected, implying a detection likelihood of ∼10%–30%. Thus, the non-detection of X-ray sources is consistent with the source detection threshold.

The nucleus of DF 44 does not exhibit an X-ray luminous source in its center, implying that any X-ray source is fainter than the detection threshold of $L_{0.5\text{–}8\,\mathrm{keV}} < 8 \times 10^{38}\,\mathrm{erg\,s^{-1}}$. DF 44 was also observed by the Karl G. Jansky Very Large Array (VLA) in the framework of the Faint Images of the Radio Sky at Twenty-cm (FIRST) project. The 1.4 GHz VLA FIRST image does not reveal a radio source associated with the nucleus of the galaxy with the detection threshold of 0.97 mJy. The X-ray and radio non-detections suggest that DF 44 does not host a luminous AGN, which is consistent with the low AGN occupation rate of UDGs (Kovács et al. 2020).

Based on the fundamental plane of black hole (BH) activity (Merloni et al. 2003), I derive an upper limit on the mass of an active BH that may reside in the center of DF 44. To this end, I convert the upper limit on the X-ray luminosity to the 2–10 keV band and the radio luminosity to 5 GHz. Assuming a power-law spectrum with a slope of $\Gamma = 1.7$, the 2–10 keV X-ray upper limit is $L_{2\text{–}10\,\mathrm{keV}} < 5.9 \times 10^{38}\,\mathrm{erg\,s^{-1}}$. I convert the 1.4 GHz VLA FIRST detection limit to 5 GHz assuming a power-law spectrum, $F_\nu \propto \nu^{-\alpha_\mathrm{R}}$, where the radio spectral index is $\alpha_\mathrm{R} = 0.8$ (Sikora et al. 2007). This results in a radio luminosity limit of $L_{5\,\mathrm{GHz}} < 2.2 \times 10^{35}\,\mathrm{erg\,s^{-1}}$. By utilizing the fundamental plane relation along with the X-ray and radio non-detections, I obtain an upper limit of $M_\mathrm{BH} < 1.2 \times 10^6\,M_\odot$. This limit is comparable to BH masses inferred for dwarf galaxies (Baldassare et al. 2020). However, the non-detection of an AGN is also compatible with a scenario, in which DF 44 hosts a more massive dormant, i.e., non-accreting, BH. Indeed, the low star formation rate of DF 44 implies that only low amounts of cold gas may be available to feed the BH, which, in turn, may result in low X-ray and radio luminosities even for a massive BH.

3.3. Unresolved X-Ray Emission

To qualitatively measure the X-ray emission associated with UDGs, I carry out X-ray photometry in the 0.5–8 keV band. The source aperture is defined as a circular region with a radius of 5 kpc (or 10.″05). This region should encloses the bulk of the emission from the hot gaseous component and from GC-LMXBs (van Dokkum et al. 2017). The background is extracted from circular annuli with 27.5–40 kpc (or 55″–80″).

The photometry confirms the empirical results based on the X-ray images: no statistically significant X-ray emission is detected either around DF 44 or DF X1. In the absence of detections, I compute 2σ upper limits on the X-ray luminosity of these UDGs. For DF 44 the Chandra and XMM-Newton upper limits are $<6.4 \times 10^{38}$ erg s^{-1} and $<2.0 \times 10^{38}$ erg s^{-1}, respectively. Although DF X1 is not covered by Chandra observations, the XMM-Newton upper limit is $< 1.4 \times 10^{39}$ erg s^{-1}. These values are comparable, albeit somewhat higher, than those obtained for the average population of UDGs in isolated and in galaxy cluster environments and exceed the X-ray luminosities predicted for a galaxy with a massive dark matter halo.

4. Summary and Discussion

In this work, I studied the X-ray emission arising from two archetypal UDGs, DF 44 and DF X1. Optical observations suggest that these galaxies may reside in massive dark matter halos, similar to those found around $L_\star$ galaxies. Given their low stellar mass ($M \sim 3 \times 10^8\,M_\odot$) and potentially high virial mass ($M_{\rm vir} \sim 5 \times 10^{11}\,M_\odot$), it was hypothesized that these galaxies are virtually "dark" galaxies. However, the X-ray observations presented in this Letter are inconsistent with this picture. If DF 44 and DF X1 were residing in a massive dark matter halos, they should exhibit X-ray luminosities of 6.1×10^{39} and 5.3×10^{39} erg s^{-1}. The observed 2σ upper limits on the X-ray luminosities are factors of $\sim$30 and $\sim$4 times lower than those expected for DF 44 and DF X1, respectively. The X-ray faint nature of these UDGs is consistent with the low X-ray luminosities observed for nearby dwarf galaxies, such as the Large Magellanic Cloud or M 32 (Points et al. 2001; Revnivtsev et al. 2007).

The virial masses inferred from the present X-ray analysis and from the population of GCs is contradictory: X-ray observations suggest factor of at least $\sim$5 times lower virial mass. To understand this discrepancy, I briefly discuss the importance of metallicity in the formation efficiency of GC-LMXBs and the recent re-investigation of the GC population around DF 44.

Galaxies hosting metal-poor GCs are less effective in forming LMXBs (Kundu et al. 2003). Given that DF 44 has low metallicity (Gu et al. 2018) and most of its GCs are metal-poor, it may host factor of about three times fewer GC-LMXBs than metal-rich GCs. Taking this correction at face value, the XMM-Newton upper limits are still factor of $\sim$10 times lower than the X-ray luminosity expected from a galaxy with a large GC population. In reality, the required correction is significantly lower than factor of three as the GC-LMXB luminosity function of Zhang et al. (2011) includes both metal-poor and metal-rich GCs. In addition, the low metallicity of DF 44 will not influence the $L_{\rm X}$–$M_{\rm tot}$ scaling relation, hence DF 44 and DF X1 are still expected to host a luminous gaseous halo if they reside in massive dark matter halos. Thus, the X-ray upper limits remain inconsistent with the presumed large GC population of these UDGs.

The GC population of DF 44 was recently re-investigated in Saifollahi et al. (2020), who suggested that DF 44 hosts $N = 19 \pm 5$ GC, which is only $\approx$25% of that measured by van Dokkum et al. (2017). The lower number of GCs stems from a different treatment of the spatial distribution of GCs and from a different background correction technique applied by Saifollahi et al. (2020). Given the $N_{\rm GC}$–$M_{\rm vir}$ scaling relation (Burkert & Forbes 2020), the population of $N = 19 \pm 5$ GC suggests a virial mass of $M_{\rm vir} = (9.5 \pm 2.5) \times 10^{10}\,M_\odot$. I note that this virial mass is also compatible with that obtained from the stellar velocity dispersion of DF 44 (van Dokkum et al. 2017). The low virial mass of DF 44 is comparable with the virial mass of dwarf galaxies (Read et al. 2017) and is much lower than that of $L_\star$ galaxies. While a similar follow-up study has not been carried out for the GC population of DF X1, van Dokkum et al. (2017) assumed the same correction, $N_{\rm GC} = 4N_{\rm GC,obs}$, between the total and observed number of GCs. However, as discussed in Saifollahi et al. (2020), this approach may significantly overestimate the number of GCs.

In this work, I relied on the $N_{\rm GC}$–$M_{\rm vir}$ and $L_{\rm X}$–$M_{\rm tot}$ scaling relations to constrain the total gravitating mass of UDGs. To probe whether the conclusions are affected by the accuracy and intrinsic scatter of these relations, I briefly overview these relations. The $N_{\rm GC}$–$M_{\rm vir}$ relation is extremely tight and exhibits low, 0.25 dex, scatter (Burkert & Forbes 2020). This relation and its scatter is in good agreement with similar studies that connect the virial mass with either the number of GCs or the derived mass of GCs (e.g., Harris et al. 2017). The scatter of the $L_{\rm X}$–$M_{\rm tot}$ relation is 0.5 dex (Kim & Fabbiano 2013) and its slope and normalization is in agreement with that established in Babyk et al. (2018). Given the X-ray upper limit on DF 44 and the intrinsic scatter of the above discussed scaling relations, DF 44 should be $\gtrsim 3\sigma$ and $\gtrsim 5\sigma$ outlier from the $L_{\rm X}$–$M_{\rm tot}$ and $N_{\rm GC}$–$M_{\rm vir}$ relation if it resides in a massive dark matter halo.

Overall, the lack of X-ray emission from DF 44 and DF X1 argues that they are not "dark" galaxies, but they follow the stellar mass-halo mass relation established for dwarf galaxies. Therefore, it is likely that DF 44 and DF X1 belong to the population of dwarf galaxies. This result is consistent with that established for the bulk of UDGs residing in isolated and cluster environments. Thus, it is unlikely that even a small subset of UDGs are failed $L_\star$ galaxies and suggests that UDGs comprise a single population.

I thank the referee for the constructive report. I thank Andra Stroe for helpful discussions on the radio observations of DF 44. The scientific results reported in this article are based to a significant degree on data obtained from the Chandra Data Archive and software provided by the Chandra X-ray Center (CXC) in the application package CIAO. This work uses observations obtained with XMM-Newton, an ESA science mission with instruments and contributions directly funded by ESA Member States and NASA. The National Radio Astronomy Observatory is a facility of the National Science Foundation operated under cooperative agreement by Associated Universities, Inc. Á.B. acknowledges support from the Smithsonian Institution.

ORCID iDs

Ákos Bogdán https://orcid.org/0000-0003-0573-7733

References

Abraham, R. G., & van Dokkum, P. G. 2014, PASP, 126, 55
Amorisco, N. C., & Loeb, A. 2016, MNRAS, 459, L51
Babyk, I. V., McNamara, B. R., Nulsen, P. E. J., et al. 2018, ApJ, 857, 32
Baldassare, V. F., Dickey, C., Geha, M., & Reines, A. E. 2020, ApJL, 898, L3
Burkert, A., & Forbes, D. A. 2020, AJ, 159, 56
Di Cintio, A., Brook, C. B., Dutton, A. A., et al. 2017, MNRAS, 466, L1
Gilfanov, M. 2004, MNRAS, 349, 146
Bogdán, Á, & Gilfanov, M. 2008, MNRAS, 388, 56
Bogdán, Á, & Gilfanov, M. 2011, MNRAS, 418, 1901
Goulding, A. D., Greene, J. E., Ma, C.-P., et al. 2016, ApJ, 826, 167
Gu, M., Conroy, C., Law, D., et al. 2018, ApJ, 859, 37
Harris, W. E., Blakeslee, J. P., & Harris, G. L. H. 2017, ApJ, 836, 67
HI4PI Collaboration, Ben Bekhti, N., Flöer, L., et al. 2016, A&A, 594, A116
Irwin, J. A., Athey, A. E., & Bregman, J. N. 2003, ApJ, 587, 356
Kim, D.-W., & Fabbiano, G. 2013, ApJ, 776, 116
Kovács, O. E., Bogdán, Á, & Canning, R. E. A. 2019, ApJL, 879, L12
Kovács, O. E., Bogdán, Á, & Canning, R. E. A. 2020, ApJ, 898, 164
Kundu, A., Maccarone, T. J., Zepf, S. E., & Puzia, T. H. 2003, ApJL, 589, L81
Lee, C. H., Hodges-Kluck, E., & Gallo, E. 2020, MNRAS, 497, 2759
Merloni, A., Heinz, S., & di Matteo, T. 2003, MNRAS, 345, 1057
Points, S. D., Chu, Y. H., Snowden, S. L., & Smith, R. C. 2001, ApJS, 136, 99
Read, J. I., Iorio, G., Agertz, O., & Fraternali, F. 2017, MNRAS, 467, 2019
Revnivtsev, M., Churazov, E., Sazonov, S., Forman, W., & Jones, C. 2007, A&A, 473, 783
Saifollahi, T., Trujillo, I., Beasley, M. A., Peletier, R. F., & Knapen, J. H. 2020, arXiv:2006.14630
Sandage, A., & Binggeli, B. 1984, AJ, 89, 919
Schombert, J. M., Bothun, G. D., Schneider, S. E., & McGaugh, S. S. 1992, AJ, 103, 1107
Sikora, M., Stawarz, Ł., & Lasota, J.-P. 2007, ApJ, 658, 815
van Dokkum, P., Abraham, R., Brodie, J., et al. 2016, ApJL, 828, L6
van Dokkum, P., Abraham, R., Romanowsky, A. J., et al. 2017, ApJL, 844, L11
van Dokkum, P., Wasserman, A., Danieli, S., et al. 2019, ApJ, 880, 91
van Dokkum, P. G., Abraham, R., Merritt, A., et al. 2015, ApJL, 798, L45
Zhang, Z., Gilfanov, M., Voss, R., et al. 2011, A&A, 533, A33